Scripta Materialia 187 (2020) 301–306

Contents lists available at ScienceDirect

Scripta Materialia

journal homepage: www.elsevier.com/locate/scriptamat

Viewpoint set

Improved fatigue resistance of gradient nanograined metallic materials: Suppress strain localization and damage accumulation

Qingsong Pan, Lei Lu*

Shenyang National Laboratory for Materials Science, Institute of Metal Research, Chinese Academy of Sciences, Shenyang 110016, People's Republic of China

ARTICLE INFO

Article history:
Received 25 March 2020
Revised 1 May 2020
Accepted 12 June 2020
Available online 24 June 2020

Keywords:
Gradient nanograin
Fatigue property
Strain delocalization
Gradient cyclic deformation
Fatigue crack

ABSTRACT

Compared to conventional metals with homogeneous microstructures, heterogeneously structured materials with spatially gradient nanostructures exhibit superior mechanical properties, especially enhanced fatigue resistance under cyclic loading by suppressing the strain localization and damage accumulation. In this paper, the basic features of fatigue properties, cyclic deformation, and damage mechanism of gradient nanostructured metallic materials are reviewed. The challenges and prospects on exploring fatigue resistance of gradient nanostructured materials in the future are also addressed.

Most structural components in service usually suffer from fatigue failure under alternating loads at very small level of cyclic stress amplitudes ($\Delta\sigma/2$) or total strain amplitudes ($\Delta\varepsilon_t/2$), which has been regarded as an everlasting unavoidable materials problem [1,2]. Comparing with the monotonic tensile test, the salient feature of fatigue is that the cyclically deformed materials undergo very small plastic strain amplitudes (i.e. $\Delta\varepsilon_{pl}/2$) which are almost comparable to the elastic strain amplitudes ($\Delta\varepsilon_e/2$) [1]. For conventional coarse grained (CG) metals under cyclic loading, cyclic plastic microstrain randomly occurs in the very local regions such as grains with soft orientation (referred to as the strain localization), which is fundamentally distinct from the feature of macro uniform plastic deformation of all grains in the metals with strains in several tens percent under uniaxial tensile tests [1,3]. However, after several thousand fatigue cycles, the accumulation of even very small irreversible plastic microstrains can be very large, being three orders of magnitude higher than the tensile strain [1]. Such a huge cumulative plastic strain inevitably results in severe inner microstructural changes, such as persistent slip bands [4–6] and locally surface roughening in the form of micron-scale extrusions in fatigued monocrystal and CG metals [3], and can thereby lead to inferior high-cycle fatigue resistance [1,7].

Extensive studies over the past three decades indicate that homogeneously refining CG into the ultrafine or nanoscale can improve the high-cycle fatigue resistance of metals, to some extent, owing to their high strengths [8–10]. However, the corresponding ultrafine grained (UFG) and nanograined (NG) metallic materials prevalently exhibit much shorter low-cycle fatigue lives and continuous cyclic softening, compared to their homogeneous CG counterparts [11–13], that greatly impede their technological application. Such inferior fatigue resistance primarily originates from the intrinsic microstructural instability of UFGs and NGs with high density defects and the severe strain localization mechanisms [9,14–16]. In particular, macroscopic shear banding and abnormal grain coarsening randomly occur in very local regions of nanostructured metals with relatively softer orientation or larger grain size [14,17,18]. Hence, developing strategies to further improve the fatigue resistance of high strength metals has become vital to the prospects from both materials science research and their engineering applications in reality.

Unique structural gradients with built-in grain sizes from nanoscale in surface to CG in core in metallic materials, hereafter named as the gradient nanograined (GNG) structures as shown in Fig. 1a, have attracted increasingly worldwide interests, due to their superior mechanical properties, such as high strength, good uniform tensile strain and extra work hardening, in comparison to their non-gradient counterparts [19–21]. Most impressively, superior fatigue behaviors have also been reported in numerous GNG metallic materials, including elevated fatigue limit under stress control and desirable fatigue life under strain control, which are rarely achieved in any of their non-gradient counterparts [22–25].

Nevertheless, despite the rapid advance made in recent years, fundamental understanding of the fatigue behavior of gradient nanostructured metallic materials is still in its infancy. Essen-

* Corresponding author.
E-mail address: llu@imr.ac.cn (L. Lu).

https://doi.org/10.1016/j.scriptamat.2020.06.038
1359-6462/

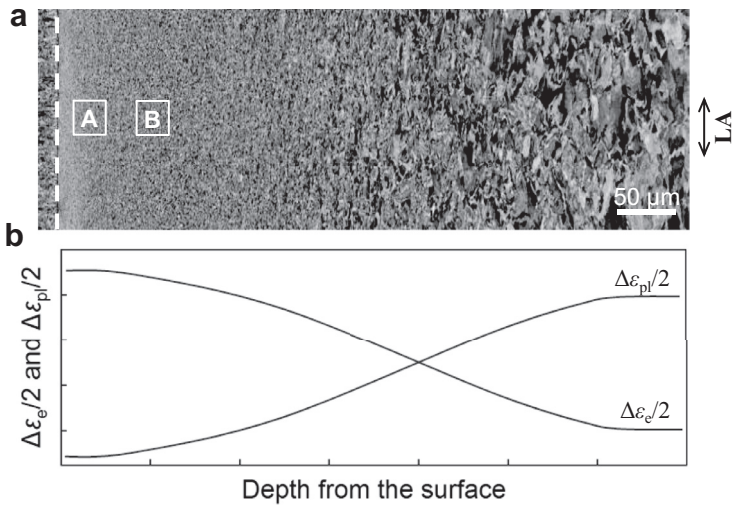

Fig. 1. Cross-sectional SEM image of gradient nanograined Cu sample (**a**). The white dashed line in (**a**) represents the treated surface; The double arrow denotes the cyclic loading axis (LA). The cyclic straining feature in different layers (i.e. inset A and B) of the gradient nanostructure with different grain sizes will be schematically illustrated in Fig. 6. (b) Schematic showing the resultant both elastic strain amplitude ($\Delta\varepsilon_e/2$) and plastic strain amplitude ($\Delta\varepsilon_{pl}/2$) are gradiently distributed along the depth from surface under cyclic loading.

tially, the gradient nanostructure under low-amplitude cyclic loading should inherently possess a unique feature of cyclic straining, introduced as following. During cyclic loading at constant $\Delta\varepsilon_t/2$, the sum of $\Delta\varepsilon_{pl}/2$ and $\Delta\varepsilon_e/2$ is maintained constant along the depth:

$$\Delta\varepsilon_t/2 = \Delta\varepsilon_e/2 + \Delta\varepsilon_{pl}/2 \quad (1)$$

In general, $\Delta\varepsilon_e/2$ is proportionally related to the stress amplitude $\Delta\sigma/2$ via Hooke's law

$$\Delta\varepsilon_e/2 = \Delta\sigma/2/E \quad (2)$$

where E is the Young's modulus (120 GPa for Cu). Distinct from the traditional cyclic strain localization in homogeneous structures with the randomly distributed elastic and plastic strain amplitudes [1], both gradient elastic and plastic strain amplitudes are resulted in GNG materials along the depth in fatigue tests at small $\Delta\varepsilon_t/2$, as schematically shown in Fig. 1b. This is because the top surface layer with finer grain size and higher stress (also the highest $\Delta\sigma/2$) deforms elasticallywhile the subsurface layers deform plastically due to their larger grains and relatively lower strength at small strain amplitude. Consequently, such resultant elastic and plastic strain gradient contribute to a novel fatigue response in the GNG structures.

In the following section, the current states-of-the-arts studies on fatigue performance of GNG metallic materials will be reviewed, including the stress- and strain- controlled fatigue properties, surface damage accumulation and cracking behavior. In particular, the novel fatigue features including the progressive yielding, plastic strain propagation, as well as several unique fatigue mechanisms will be considered. The challenges and prospects on fatigue resistance of the gradient nanostructured materials are addressed as well.

Basic fatigue properties and mechanisms of gradient nanostructure

Both stress- and strain- controlled tension-compression tests at room temperature have been commonly carried out to investigate the fatigue responses of GNG metallic materials prepared by means of surface plastic deformation treatment, such as surface mechanical grinding/rolling treatment [24–26], laser/ultrasonic shock peening [27–30]. Fig. 2a summaries the stress amplitude, $\Delta\sigma/2$, versus fatigue life, N_f (i.e. *S-N* curves) of GNG Cu[24], 316 SS[25], 304 SS [27] and Ti alloy (Ti–6Al–4V) [28] under stress control using sinusoidal wave form loading profile. Obviously, GNG structures exhibit superior fatigue resistance under high-cycle fatigue tests, comparable to that of UFG and NG counterparts, and much better than that of CG counterparts [7,16,31]. Taken GNG Cu as a typical instance, its fatigue life is at least ten times longer than that of CG Cu fatigued at the same $\Delta\sigma/2$. Its fatigue endurance limit is almost twice that of CG and nearly comparable to that of UFG counterparts [8,32,33]. Evidently, the high tensile strength of GNG metals, owing to the presence of high-strength GNG surface layers, benefits for the enhanced stress-controlled fatigue properties, analogous to that of homogeneous nanostructured metals [2,9].

To preclude the contribution of the strength itself to high-cycle fatigue properties, the fatigue ratio, as another key fatigue parameter, is defined as the ratio of $\Delta\sigma/2$ to the ultimate tensile strength (σ_{UTS}) of metal, which can reflect the structural resistance to stress-controlled fatigue preferably [1,24]. Fig. 2b shows the fatigue ratio plotted against N_f (i.e. the normalized *S-N* data in Fig. 2a). GNG structures exhibit the highest fatigue ratio, comparing to the non-gradient counterpart at the same N_f. The stress ratio of GNG Cu at 10^7 cycles is 0.4, which is about twice that for homogeneous CG and for most of UFG Cu reported in literature [8,32,33]. Similar fatigue trend is also detected in both GNG 316 SS and 304 SS (Fig. 2b).

Fig. 3a displays the typical cyclic stress (i.e. $\Delta\sigma/2$) response of GNG Cu and 316 SS at constant $\Delta\varepsilon_t/2$ of 0.5%, which was controlled by a dynamic strain gauge extensometer with a total strain rate of 0.2–0.5% s^{-1} [24,26]. Owing to the presence of high-strength GNG layer, both GNG specimens exhibit elevated $\Delta\sigma/2$, compared with CG at the same $\Delta\varepsilon_t/2$. Especially, a unique cyclic stability with nearly constant $\Delta\sigma/2$ is maintained in GNG Cu after a short initial hardening stage, which is distinct from the continuous cyclic hardening of CG Cu [1,34]. In contrast, the cyclic response of GNG 316 SS is much analogous to that of CG counterpart, except for the appearance of distinct secondary hardening in the late stage of fatigue tests [26]. The cyclic responses of GNG materials in Fig. 3a are the collective and integrated effects of cyclic behaviors of GNG surface layer and CG core, which are fundamentally different from the typical continuous cyclic softening universally detected in various nanostructured metallic materials under strain controlled fatigue tests [11,13,31].

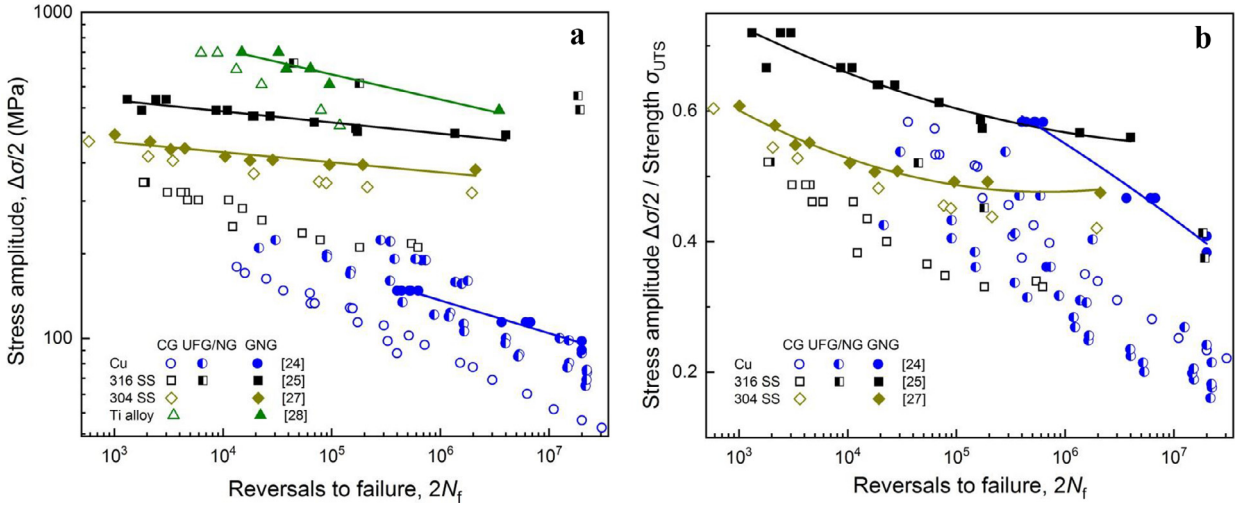

Fig. 2. High-cycle fatigue properties of GNG metallic materials under stress control. Dependence of high-cycle fatigue life (N_f) on stress amplitude ($\Delta\sigma/2$) (**a**) and on the normalized stress amplitude ($\Delta\sigma/2$) by the ultimate tensile strength (σ_{UTS}) (**b**), respectively. For comparison, $\Delta\sigma/2$ versus N_f data of their homogeneous CG, UFG and NG conterparts are also included [7,16,31].

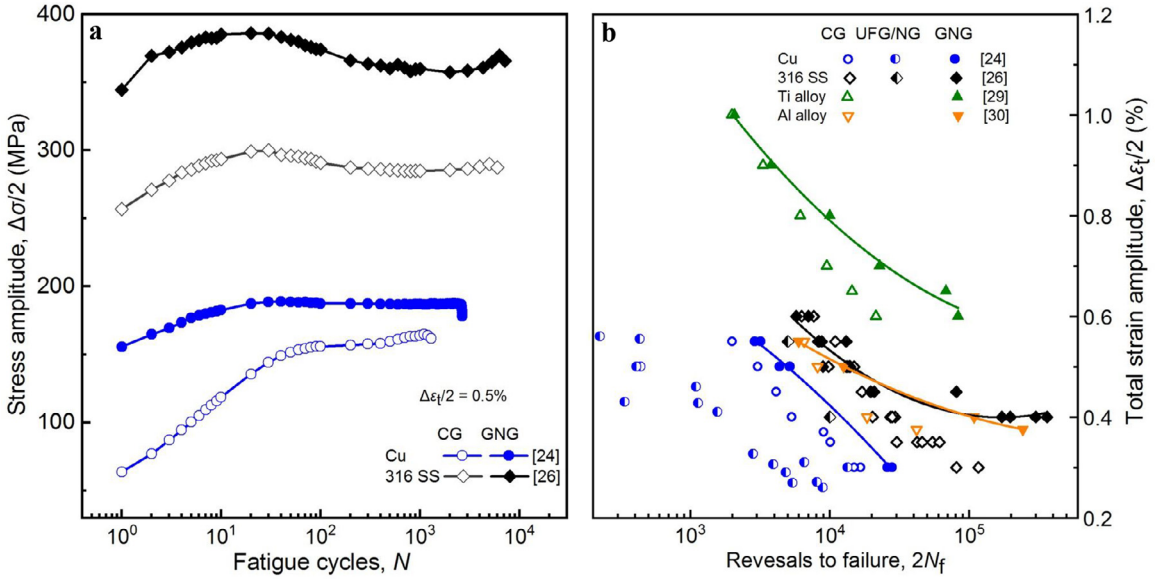

Fig. 3. Low-cycle fatigue properties of GNG metallic materials under strain control. (**a**) Typical cyclic stress response ($\Delta\sigma/2$) of GNG Cu and 316 SS at a typical $\Delta\varepsilon_t/2$ of 0.5%. Dependence of fatigue life (N_f) on $\Delta\varepsilon_t/2$ of GNG metals (**b**). For comparison, $\Delta\varepsilon_t/2$ versus *Nf* data of their non-gradient conterparts are also included [24,26,29–31].

The total strain amplitude versus fatigue life curves of GNG Cu [24], 316 SS [26], Ti alloy [29] and 2014 Al alloys [30] under strain controlled fatigue are summarized in Fig. 3b. It is well accepted that CG metals display the longest strain-controlled low-cycle fatigue life among the homogeneous structures, like CG, UFG and NG, owing to their desirable ductility [9,14,24]. Surprising, the low-cycle fatigue lifetimes of GNG materials are even longer at the same $\Delta\varepsilon_t/2$.

Above results in Figs. 2 and 3 explicitly demonstrate that "coating" CG with a spatial gradient nanostructure skin can significantly enhance the fatigue resistance in both low- and high-cycle fatigue regimes, i.e. longer fatigue life and higher stress amplitude (especially fatigue limit), which are much better than any individual non-gradient counterpart.

Most fatigue crack initiation occurs on the free surface, as a result of surface damage accumulation and roughening, like extrusions in CG [1,35] and shear bands in nanostructured metals during cyclic loading [14]. In order to enhance fatigue resistance, suppressing surface roughening and cracking are recognized as effective and necessary approaches. Typical SEM image of GNG Cu after repeated loading until failure at very large $\Delta\varepsilon_t/2 = 0.5\%$ in Fig. 4a indeed shows relatively smooth surface with only a few damage features. The surface fluctuation in GNG Cu (~160 nm) is at least one order of magnitude smaller than the micron-scale extrusions of fatigued homogeneous CG counterparts (Fig. 4b–d) [24].

When the second phase strengthened alloys such as ferritic-martensitic dual phase (DP) steels under cyclic loading, the cracks initiate in the vicinity of interfaces preferentially between soft ferrite and hard matensite phases on surface (Fig. 4f), owing to the severe cyclic strain incompatibility and stress concentration [36]. In contrast, both phases on the surface of GNG DP steels are extremely refined and have comparable high strengths [37]. During subsequent cyclic loading, nucleation of fatigue cracks at phase interfaces in gradient nanostructures can be substantially suppressed, which results in strong resistance to high-cycle fatigue (Fig. 4c) [26,37].

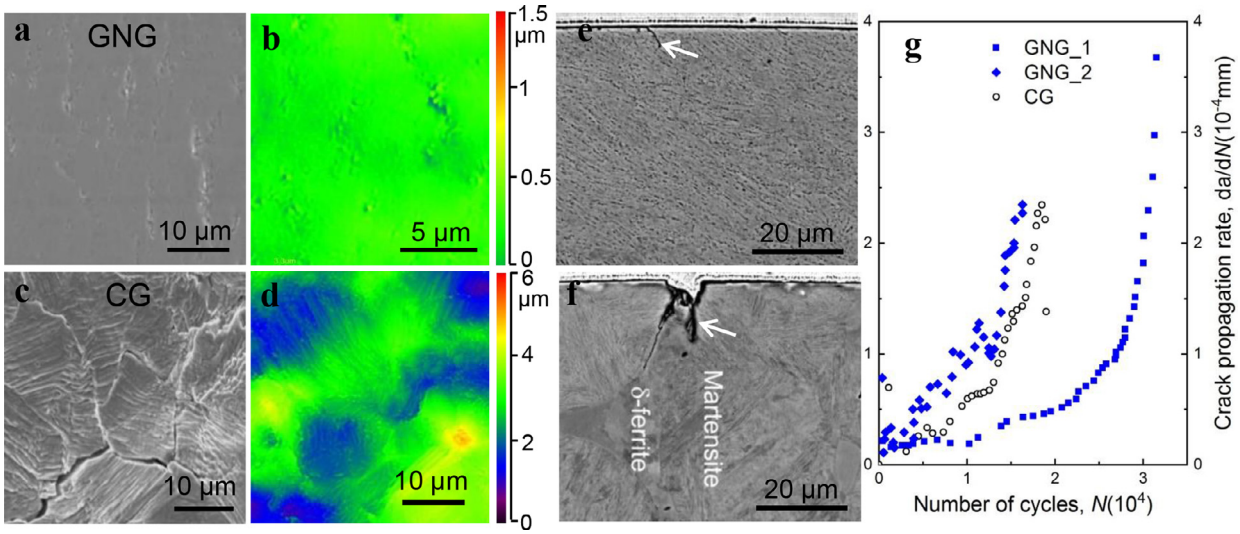

Fig. 4. Suppressed surface damage accumulation and cracking behavior of GNG materials. Typical SEM and confocal laser scanning microscopy images on the surface of GNG Cu (**a, b**) and CG Cu (**c, d**) after failure at $\Delta\varepsilon_t/2$ of 0.5% [24].The contrast in **b** and **d** indicates the height variation in surface roughness morphology measured by the color bar on the right. Typical fatigue crack in GNG (**e**) and CG dual phase steel (**f**) after fatigue tests [37]; (**g**) Fatigue crack propagation rate (da/dN) as a function of number of cycles in GNG and CG steels [38].

Apart from the substantial suppression of surface damage accumulation and crack initiation, the gradient nanostructure also enhances the resistance to fatigue crack propagation by altering the stress/strain distribution around the crack tip. Fig. 4g shows an example of the fatigue crack propagation rate in one GNG 304 steel under three-point bending tests [38]. The GNG_1 sample with pre-crack in CG core exhibits a better resistance to fatigue crack propagation from CG to nanostructure than the other one with an inverse propagation direction (GNG_2 with pre-crack in GNG layer) and CG, which remarkably differs from the reduced resistance to fatigue crack propagation in homogeneous UFG and NG metals [14,39]. This arises from the existence of more homogeneous stress field and the lower stress/strain concentration ahead of the crack tip in the gradient structure of GNG_1 sample, compared to GNG_2 counterpart [38,40].

Consider GNG Cu as a typical example, we summarize the variations of measured grain size, hardness (H_v), estimated elastic, plastic and accumulated plastic strains along the depth from the surface during fatigue tests in Fig. 5 (see details in [24]). With increasing the number of cycles (N), grain coarsening occurs [24], which contributes to the progressive homogenization of an initially gradient nanostructure (Fig. 5a). The average size of both grains in GNG layer and the dislocation patterns in CG core converges to an identical value, approximately 1 μm, i.e. a steady-state microstructure emerges upon cyclic loading [24]. Correspondently, H_v of the top surface GNG layer gradually decreases with increasing cycles, such that at $N = N_f$, the final hardness in the whole GNG layer becomes approximately comparable to that in CG core (Fig. 5b)

Ordered, progressive plastic yielding and elastic-plastic deformation transformation is also detected in the gradient nanostructure during cyclic deformation [24]. In the very first cycles at $\Delta\varepsilon_t/2$ of 0.5%, the topmost surface of GNG Cu possesses the largest $\Delta\varepsilon_e/2$ of ~0.5%, which then monotonically reduces along depth to about 0.15% in CG core (Fig. 5c). Nevertheless, $\Delta\varepsilon_{pl}/2$ exhibits an opposite profile with almost zero in the topmost layer and the largest value in the core (~0.35%), as shown in Fig. 5d. With increasing the number of cycles, a monotonic drop of $\Delta\varepsilon_e/2$ is detected in GNG layer while slightly increment of $\Delta\varepsilon_e/2$ occurs in core (Fig. 5c). On the contrary, $\Delta\varepsilon_{pl}/2$ gradually increases in GNG layer (Fig. 5d). That suggests that the cyclic plastic strain with a large $\Delta\varepsilon_{pl}/2$ progressively propagates from CG toward to surface. Finally at failure, the topmost layer accommodates a comparable $\Delta\varepsilon_{pl}/2$ to that in CG core.

Likewise, the cumulative plastic strain ($\Sigma 4\Delta\varepsilon_{pl}/2$) monotonically increases in GNG layer during the whole fatigue stage, as shown in Fig. 5e. Notably, an unusually large cumulative cyclic plastic strain, as high as 20–35, accumulates in GNG Cu, which is much larger than that which can be achieved in homogeneous CG Cu (~20) and UFG Cu (several) at the same fatigue conditions [1,24].

The foregoing analysis evidently demonstrates that the progressive propagation of the spatially distributed cyclic strain amplitudes (including both $\Delta\varepsilon_e/2$ and $\Delta\varepsilon_{pl}/2$) are inherent in the built-in gradient nanostructures under small amplitude cyclic loading. Hysteresis loop variations of two typical layers with different grains, i.e. inset A and B in Fig. 1a, are schematically re-illustrated as a function of fatigue cycles in Fig. 6. Obviously, cyclic plastic strain is observed initially in the soft B layer with larger grains, which occurs prior to that of the stronger A layer with smaller grain size and higher cyclic stress. With increasing the cyclic numbers, plastic strain gradually propagates to the A layer, and finally evolves with almost the same hysteresis loop as that in the B layer. Such salient features of progressive yielding (or plastic deformation) and strain-delocalized fatigue behavior in gradient nanostructure are fundamentally distinct from the cyclic strain localization, which randomly locates in sparse regions of conventional non-gradient counterparts under cyclic loading [1,3,14].

The structure gradient also induces some novel cyclic mechanisms in the GNG metallic materials, which do not exist in the non-gradient counterparts. For example, either homogeneous or abnormal grain coarsening, which closely depends on the imposed strain amplitude, dominates the cyclic mechanism of GNG Cu [41,42]. An enhanced martensitic transformation, acting as a new carrier to accommodate a higher cyclic plastic strain, is also detected in cyclically deformed GNG 316 SS [26]. But, the strain localization universally seen in UFG and NG metals, such as macroscopic shear banding [14,43,44], is not observed in cyclically deformed GNG metals [24,26].

Such unique strain-delocalized cyclic mechanisms in GNG structure thereby impart an unprecedented resistance to both low-cycle and high-cycle fatigues, as shown in Figs. 1–4. Furthermore, increasing the GNG volume fraction of GNG Cu can efficiently elevate

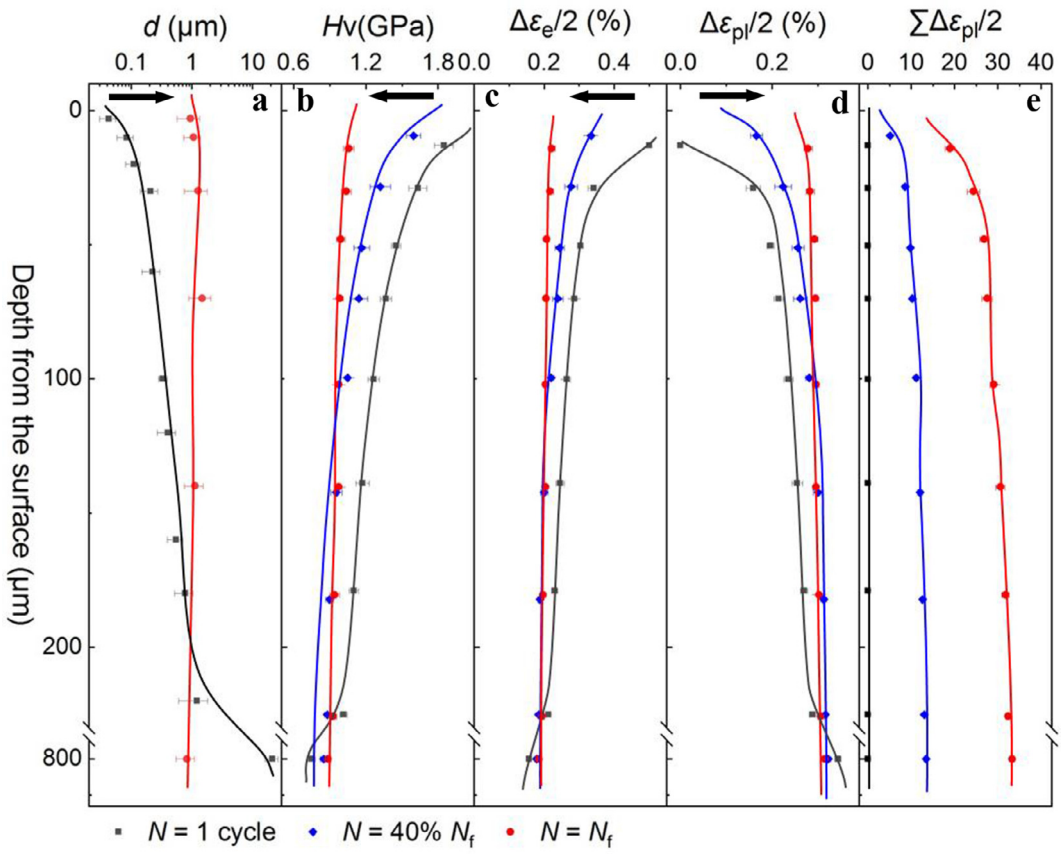

Fig. 5. Typical resultant gradient features induced by the built-in gradient nanograined Cu under cyclic deformation. The variations of measured average grain size d (a), microhardness Hv (b), the estimated elastic strain amplitude $\Delta\varepsilon_e/2$ (c), plastic strain amplitude $\Delta\varepsilon_{pl}/2$ (d) and cumulative plastic strain $\Sigma\Delta\varepsilon_{pl}/2$ (e) along the distance from the top surface to interior as a function of cycles at $\Delta\varepsilon_t/2 = 0.5\%$. The arrows in a-d represent the evolution trend of d, Hv, $\Delta\varepsilon_e/2$ and $\Sigma\Delta\varepsilon_{pl}/2$ with the number of cycles, respectively.

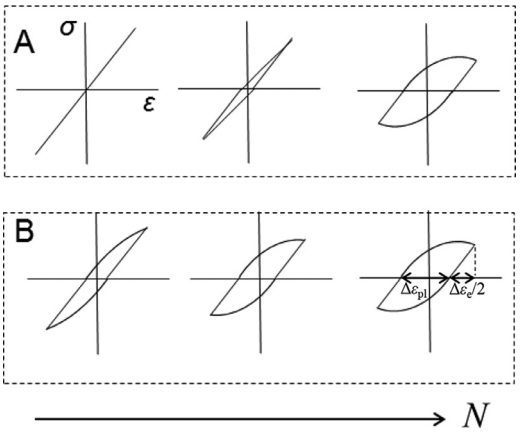

Fig. 6. Schematic of cyclic straining feature of GNG materials, showing that the gradient nanostructure displays different types of hysteresis loops in different layers, which also gradually vary during cyclic loading. A: strong layer with a small grain size; B: soft layer with a relatively larger grain size (inset in Fig. 1a).

the high-cyclic fatigue limit, by remarkably postponing the abnormal grain coarsening from the deeper subsurface layer to the topmost surface [45]. But, it does not influence the low-cycle fatigue life significantly [46].

The residual compressive stress induced in gradient nanostructures during surface plastic deformation treatment is another non-negligible factor on tuning the fatigue resistance of GNG materials. A longer high-cycle fatigue life can be achieved in GNG Cu with a higher residual stress, compared to that of the annealed GNG Cu with similar gradient microstructure but having relative reduced residual stress [47]. The enhanced high-cycle fatigue resistance arises from the slower accumulation of plastic strain in GNG layer and the arrested crack initiation caused by residual compressive stress. However, such beneficial effect on low-cycle fatigue resistance of GNG metals may be limited, given the strain delocalization associated with homogeneous grain coarsening and the rapid release of residual stress in very short early cycles when cyclically deformed at very large-amplitude cyclic straining [26].

Concluding remarks and perspective

To conclude, a gradient nanostructure skin covering CG substrate can greatly enhance both low-cycle and high-cycle fatigue resistances of several GNG metallic materials, as opposed to the traditional trade-off between low-cycle and high-cycle fatigue properties universally reported in conventional homogeneous CG and nanostructure materials. Such all-round superior fatigue resistance essentially arises from the de-localized cyclic deformation associated with the spatially gradient distributed cyclic elastic and plastic strains, and their ordered, progressive transmission in the gradient nanostructure during cyclic loading. Although some advances in the fatigue behavior of GNG metallic materials have been achieved, there are still numerous critical issues that need to be addressed.

Regarding to trans-scale gradient nanograined structures in metallic materials, decoupling their multiple microstructural parameters (such as grain size, grain geometry, distribution and vol-

ume fraction) and residual stress effects on fatigue resistance and cracking behavior provides new opportunities and challenge for experimental, analytical and simulation studies. Besides, fatigue damage resistance of other typical heterogeneous microstructures, such as gradient nanolayer, gradient nanotwins, dual gradient structure with grain size and twin thickness, are still intriguing unexplored issues. In particular, the geometrically necessary dislocations are supposed to accommodate the plastic deformation incompatibility and strain gradient induced by gradient structures [48–50]. However, their morphologies (if exist) as well as the role they played on the cyclic straining and fatigue response of various gradient nanostructures are rarely reported and, worthy of in-depth study. The quantifying correlations among hierarchical gradient nanostructures, fatigue property and cyclic mechanism will advance the potential engineering application and tailor-designing of new fatigue-resistant materials.

Declaration of Competing Interest

The authors declare that they have no known competing financial interests or personal relationships that could have appeared to influence the work reported in this paper.

Acknowledgements

The authors acknowledge financial support by National Science Foundation of China (NSFC, Grant Numbers. U1608257 and 51931010), the Key Research Program of Frontier Science and International partnership program (Grant Number. GJHZ2029), CAS, and LiaoNing Revitalization Talents Program (Grant Number. XLYC1802026). Q.P. acknowledges support by NSFC (Grant Number. 51601196) and Youth Innovation Promotion Association CAS (Grant Number. 2019196).

References

[1] S. Suresh, Fatigue of Materials, second ed., Cambridge University Press, Cambridge, 1998.
[2] H. Mughrabi, Proc. Eng. 2 (2010) 3–26.
[3] P. Peralta, C. Laird, D.E. Laughlin, K. Hono, Fatigue of Metals, Physical Metallurgy, fifth ed., Elsevier, Oxford, 2014, pp. 1765–1880.
[4] H. Mughrabi, Philos. Trans. A (2015) 373.
[5] J.A. Ewing, J.C.W. Humfrey, Philos. Trans. R. Soc. A 200 (1903) 241–250.
[6] Z.S. Basinski, S.J. Basinski, Prog. Mater. Sci. 36 (1992) 89–148.
[7] A.W. Thompson, W.A. Backofen, Acta Metall. 19 (1971) 597–606.
[8] H. Mughrabi, H.W. Höppel, M. Kautz, Scr. Mater. 51 (2004) 807–812.
[9] A. Pineau, A. Amine Benzerga, T. Pardoen, Acta Mater. 107 (2016) 508–544.
[10] L. Kunz, P. Lukáš, A. Svoboda, Mater. Sci. Eng. A 424 (2006) 97–104.
[11] H.W. Höppel, Z.M. Zhou, H. Mughrabi, R.Z. Valiev, Philos. Mag. A 82 (2002) 1781–1794.
[12] A. Vinogradov, S. Hashimoto, Mater. Trans., JIM 42 (2001) 74–84.
[13] S.R. Agnew, J.R. Weertman, Mater. Sci. Eng. A 244 (1998) 145–153.
[14] H. Mughrabi, H.W. Höppel, Int. J. Fatigue 32 (2010) 1413–1427.
[15] Q.S. Pan, H.F. Zhou, Q.H. Lu, H.J. Gao, L. Lu, Nature 551 (2017) 214–217.
[16] Q.S. Pan, L. Lu, Acta Mater. 81 (2014) 248–257.
[17] M. Goto, K. Kamil, S.Z. Han, K. Euh, S.S. Kim, J. Lee, Int. J. Fatigue 51 (2013) 57–67.
[18] T.A. Furnish, A. Mehta, D. Van Campen, D.C. Bufford, K. Hattar, B.L. Boyce, J. Mater. Sci. 52 (2017) 46–59.
[19] T.H. Fang, W.L. Li, N.R. Tao, K. Lu, Science 331 (2011) 1587–1590.
[20] X.L. Wu, P. Jiang, L. Chen, F.P. Yuan, Y.T.T. Zhu, Proc. Natl. Acad. Sci. USA 111 (2014) 7197–7201.
[21] Y.J. Wei, Y.Q. Li, L.C. Zhu, Y. Liu, X.Q. Lei, G. Wang, Y.X. Wu, Z.L. Mi, J.B. Liu, H.T. Wang, H.J. Gao, Nat. Commun. 5 (2014) 3580.
[22] T. Roland, D. Retraint, K. Lu, J. Lu, Scr. Mater. 54 (2006) 1949–1954.
[23] J.W. Tian, J.C. Villegas, W. Yuan, D. Fielden, L. Shaw, P.K. Liaw, D.L. Klarstrom, Mater. Sci. Eng. A 468 (2007) 164–170.
[24] J.Z. Long, Q.S. Pan, N.R. Tao, M. Dao, S. Suresh, L. Lu, Acta Mater. 166 (2019) 56–66.
[25] H.W. Huang, Z.B. Wang, J. Lu, K. Lu, Acta Mater. 87 (2015) 150–160.
[26] Y.B. Lei, Z.B. Wang, J.L. Xu, K. Lu, Acta Mater. 168 (2019) 133–142.
[27] I. Nikitin, B. Scholtes, H.J. Maier, I. Altenberger, Scr. Mater. 50 (2004) 1345–1350.
[28] R.K. Nalla, I. Altenberger, U. Noster, G.Y. Liu, B. Scholtes, R.O. Ritchie, Mater. Sci. Eng. A 355 (2003) 216–230.
[29] S. Kumar, K. Chattopadhyay, V. Singh, J. Alloy. Compd. 724 (2017) 187–197.
[30] V. Pandey, G.S. Rao, K. Chattopadhyay, N.C. Santhi Srinivas, V. Singh, Mater. Sci. Eng. A 647 (2015) 201–211.
[31] H. Ueno, K. Kakihata, Y. Kaneko, S. Hashimoto, A. Vinogradov, Acta Mater. 59 (2011) 7060–7069.
[32] P. Lukáš, L. Kunz, M. Svoboda, Kovove Mater. 47 (2009) 1–9.
[33] P. Xue, Z.Y. Huang, B.B. Wang, Y.Z. Tian, W. Wang, B.L. Xiao, Z.L. Ma, Sci. China Mater. 59 (2016) 1–7.
[34] J. Polák, M. Klesnil, Mater. Sci. Eng. 63 (1984) 189–196.
[35] N. Thompson, N. Wadsworth, N. Louat, Philos. Mag. 1 (1956) 113–126.
[36] Z.G. Wang, G.N. Wang, W. Ke, H.C. He, Mater. Sci. Eng. 91 (1987) 39–44.
[37] H.W. Huang, Z.B. Wang, X.P. Yong, K. Lu, Mater. Sci. Technol. 29 (2013) 1200–1205.
[38] Z.W. Ma, J.B. Liu, G. Wang, H.T. Wang, Y.J. Wei, H.J. Gao, Sci. Rep. 6 (2016) 22156.
[39] T. Hanlon, Y.N. Kwon, S. Suresh, Scr. Mater. 49 (2003) 675–680.
[40] Y. Wang, L.C. Yuan, S.J. Zhang, C.Q. Sun, W.J. Wang, G.X. Yang, Q. Li, Y.J. Wei, Eng. Fract. Mech. 209 (2019) 369–381.
[41] J.Z. Long, Q.S. Pan, N.R. Tao, L. Lu, Scr. Mater. 145 (2018) 99–103.
[42] Q.S. Pan, J.Z. Long, L.J. Jing, N.R. Tao, L. Lu, Under revision, (2020).
[43] S.D. Wu, Z.G. Wang, C.B. Jiang, G.Y. Li, I.V. Alexandrov, R.Z. Valiev, Scr. Mater. 48 (2003) 1605–1609.
[44] M. Goto, S.Z. Han, T. Yakushiji, C.Y. Lim, Kim, Scr. Mater. 54 (2006) 2101–2106.
[45] L.J. Jing, Q.S. Pan, J.Z. Long, N.R. Tao, L. Lu, Scr. Mater. 161 (2019) 74–77.
[46] L.J. Jing, Q.S. Pan, L. Lu, Adv. Eng. Mater. (2019) 1900554.
[47] J.Z. Long, Q.S. Pan, N.R. Tao, L. Lu, Mater. Res. Lett. 6 (2018) 456–461.
[48] M.F. Ashby, Philos. Mag. 21 (1970) 399–424.
[49] N.A. Fleck, G.M. Muller, M.F. Ashby, J.W. Hutchinson, Acta Metall. Mater. 42 (1994) 475–7487.
[50] H.J. Gao, Y.G. Huang, W.D. Nix, J.W. Hutchinson, J. Mech. Phys. Solids 47 (1999) 1239–1263.